



**HAL**  
open science

## From transglutaminases (TGs) to arylamine N-acetyltransferases (NATs): Insight into the role of a spatially conserved aromatic amino acid position in the active site of these two families of enzymes

Ximing Xu, Wenchao Zhang, Jeremy Berthelet, Rongxing Liu, Christina Michail, Alain F. Chaffotte, Jean-Marie Dupret, Fernando Rodrigues-Lima

### ► To cite this version:

Ximing Xu, Wenchao Zhang, Jeremy Berthelet, Rongxing Liu, Christina Michail, et al.. From transglutaminases (TGs) to arylamine N-acetyltransferases (NATs): Insight into the role of a spatially conserved aromatic amino acid position in the active site of these two families of enzymes. *Biochemical and Biophysical Research Communications*, 2020, 525 (2), pp.308-312. 10.1016/j.bbrc.2020.02.082 . hal-03300412

**HAL Id: hal-03300412**

**<https://cnrs.hal.science/hal-03300412>**

Submitted on 20 May 2022

**HAL** is a multi-disciplinary open access archive for the deposit and dissemination of scientific research documents, whether they are published or not. The documents may come from teaching and research institutions in France or abroad, or from public or private research centers.

L'archive ouverte pluridisciplinaire **HAL**, est destinée au dépôt et à la diffusion de documents scientifiques de niveau recherche, publiés ou non, émanant des établissements d'enseignement et de recherche français ou étrangers, des laboratoires publics ou privés.



Distributed under a Creative Commons Attribution - NonCommercial 4.0 International License

**From transglutaminases (TGs) to arylamine *N*-acetyltransferases (NATs): Insight into the role of a spatially conserved aromatic amino acid position in the active site of these two families of enzymes**

Ximing Xu<sup>1, 2, #</sup>, Wenchao Zhang<sup>1, #</sup>, Jérémy Berthelet<sup>1</sup>, Rongxing Liu<sup>1</sup>, Christina Michail<sup>1</sup>, Alain F. Chaffotte<sup>3</sup>, Jean-Marie Dupret<sup>1</sup> and Fernando Rodrigues-Lima<sup>1, \*</sup>

<sup>1</sup> Université de Paris, BFA, UMR 8251, CNRS, F-75013, Paris, France

<sup>2</sup> Key Laboratory of Marine Drugs, Chinese Ministry of Education, School of Medicine and Pharmacy, Ocean University of China, Qingdao, 266003, China

<sup>3</sup> Institut Pasteur, Unité de Résonance Magnétique Nucléaire des Biomolécules, Paris, France

# These authors contributed equally and should be considered as co-first authors

Correspondence : [fernando.rodrigues-lima@u-paris.fr](mailto:fernando.rodrigues-lima@u-paris.fr) (F. Rodrigues-Lima)

## **ABSTRACT**

Transglutaminases (TG) and arylamine *N*-acetyltransferases (NAT) are important family of enzymes. Although they catalyze different reactions and have distinct structures, these two families of enzymes share a spatially conserved catalytic triad (Cys, His, Asp residues). In active TGs, a conserved Trp residue located close to the triad cysteine is crucial for catalysis through stabilization of transition states.

Here, we show that in addition to sharing a similar catalytic triad with TGs, functional NAT enzymes also possess in their active site an aromatic residue (Phe, Tyr or Trp) occupying a structural position similar to the Trp residue of active TGs. More importantly, as observed in active TGs, our data indicates that in functional NAT enzymes this conserved aromatic residue is also involved in stabilization of transition states. These results thus indicate that in addition to the three triad residues, these two families of enzymes also share a spatially conserved aromatic amino acid position important for catalysis. Identification of residues involved in the stabilization of transition states is important to develop potent inhibitors. Interestingly, NAT enzymes have been shown as potential targets of clinical interest.

**Keywords:** Arylamine *N*-acetyltransferases, transglutaminases, active site, catalytic mechanism, transition state

## INTRODUCTION

Transglutaminases (TGs) (EC 2.3.2.13) are a family of calcium-dependent enzymes that catalyze the formation of an isopeptide bond between glutamine side chains and the  $\epsilon$ -amino groups of lysine residue side chains [1-3]. This process results in cross-linking of proteins involved in important biological processes such as coagulation. Crystal structures of TGs have shown that the catalytic center of these enzymes shares common structural properties with the papain-like family of cysteine protease, notably the presence of a catalytic triad of Cys-His-Asp [2,4].

Arylamine *N*-acetyltransferases (NATs) (EC 2.3.1.5) are an important family of xenobiotic-metabolizing enzymes that catalyze the acetyl-coenzyme A (AcCoA)-dependent acetylation of arylamines including drugs and carcinogens [5,6]. NAT enzymes are found in a range of eukaryotic and prokaryotic species where they may play diverse functions [6-9]. Several eukaryotic and prokaryotic NAT enzymes have been described at both functional and structural levels [9-16]. All these structural studies identified a common fold that comprises three domains and a Cys-His-Asp/Glu catalytic triad in the active site of NAT enzymes [9,14,16,17]. Although TG and NAT enzymes have otherwise distinct 3D structures, catalyze different reactions and assume different functions, the structural studies on TGs and NATs indicate that these two families of enzymes both share a catalytic center and notably a structurally conserved catalytic triad [2,18]. In addition, the catalytic reaction of TG and NAT enzymes relies on ping-pong mechanisms where the cysteine of the triad acts as the catalytic nucleophile residue [2,12,14,18,19]. Further studies on TGs identified a strictly conserved aromatic residue (corresponding to Trp 241 in human TG2) in the active site that is essential for activity of these enzymes [2,4]. This Trp residue is conserved in all enzymatically active TGs and has been shown to serve mainly on the stabilization of transition-states through interaction involving the side chain of the Trp residue [4]. By using

different structural and enzymatic approaches, we show that in addition to sharing a similar catalytic triad with TGs, NAT enzymes also possess in their active site an aromatic residue (Phe, Tyr or Trp) occupying a structural position similar to the Trp residue of functional TGs. The identification in active site of NATs of a conserved position involved in stabilization of transition states is of importance to better understand the catalytic mechanisms of this family of enzymes and to design potent inhibitors [20].

## **MATERIALS AND METHODS**

### ***Materials***

Acetyl coenzyme A (AcCoA), p-nitrophenylacetate (PNPA), p-dimethylaminobenzaldehyde (DMAB), p-aminosalicylate (PAS), 2-aminofluorene (2-AF) were from Sigma-Aldrich.

### ***Expression and purification of wild-type *Mesorhizobium loti* NAT1 and mutant enzymes***

The pET28a-*M. loti* NAT1 vector encodes the enzyme as a (6xHis) tagged fusion protein and was used as a template to make Phe42Tyr, Phe42Trp, Phe42His, Phe42Ile and Phe42Ala mutants as described previously [21]. Expression of the NAT proteins in *E. coli* BL21(DE3) and purification was carried out as reported previously [21]. Protein concentrations were determined using the Bradford assay (Bio-rad). Proteins were also analyzed by SDS-PAGE and stained using Coomassie stain.

### ***NATs activity assays***

PNPA assays were carried out in 96-well plates as described previously [8]. Briefly, the mixtures contained NAT enzyme (5  $\mu$ g/ml final) and p-AS or 2-AF (500  $\mu$ M final) in a volume of 100  $\mu$ l of 25 mM Tris-HCl pH 7.5. The reaction was initiated by addition of PNPA (2 mM final) dissolved in DMSO. The rates were determined by monitoring the increase in absorbance at 405 nm using a thermostated (37 °C) plate reader (BioTek, France). The data were corrected by subtracting the non specific hydrolysis of PNPA in the absence of NAT enzyme. All assays were done in triplicates and are shown as mean  $\pm$ SD.

DMAB assays were also carried out in 96-well plates as described previously [8]. Briefly, 50  $\mu$ L reaction mixtures, containing NAT enzyme (10  $\mu$ g/mL), *p*-AS (0-300  $\mu$ M) and AcCoA (0-400  $\mu$ M) in 25 mM Tris-HCl pH 7.5. The reaction was quenched by adding 40  $\mu$ L of cold trichloroacetic acid (40%). Finally, 100  $\mu$ L DMAB (2%) in 9:1 acetonitrile and water were added to the mixture. Reaction rate was monitored according the decrease of absorbance at 450 nm. All assays were done in triplicates and are shown as mean  $\pm$ SD.

NATs catalyze acetyl transfer using a ping pong bi-bi mechanism. Accordingly, kinetic constants for *M. loti* NAT1 (wild type) and mutants were determined by nonlinear fitting to the equation 1 or equation 2 (in case of substrate inhibition behavior at high concentration of substrates) [22]:

$$1: v = \frac{V_{\max} AB}{K_{AB} + K_{BA} + AB}$$

$$2: v = \frac{V_{\max} AB}{K_{AB}(1 + \frac{B}{K_{iB}}) + K_{BA} + AB}$$

where  $V_{\max}$  is the maximum velocity; A and B are the concentrations of the two substrates;  $K_A$  and  $K_B$  are Michaelis-Menten constants for substrate A and B, respectively.  $K_{iB}$  is the inhibition constant for *p*-AS. The overall rate constant  $k_{\text{cat}}$  was calculated by using  $k_{\text{cat}} = V_{\max}/[E_0]$ , where  $[E_0]$  is total enzyme concentration.

Thermodynamic parameters ( $\Delta\Delta G_B$  and  $\Delta\Delta G_{TS}$ ) were calculated as previously described [4,23](see equations 3 and 4) and represent, respectively, the difference between WT and mutant enzymes in free energy required to form the enzyme-substrate complex (ES) from E+S, and the difference in free energy between WT and mutants to stabilize the transition-state complex.

$$3: \Delta\Delta G_B = \Delta G_{B \text{ mut}} - \Delta G_{B \text{ wt}} = RT \ln \left( \frac{K_{m \text{ mut}}}{K_{m \text{ wt}}} \right)$$

$$4: \Delta\Delta G_{TS} = \Delta G_{TS \text{ mut}} - \Delta G_{TS \text{ wt}} = RT \ln \left[ \frac{(k_{\text{cat}} / K_m)_{\text{wt}}}{(k_{\text{cat}} / K_m)_{\text{mut}}} \right]$$

### **Circular dichroism (CD) spectroscopy**

Circular dichroism analyzes were carried out at described previously [24]. *M. loti* NAT1 and

mutants (0.5 mg/ml or 2 mg/ml) were dialyzed against 20 mM potassium phosphate buffer (pH 7.5).

### ***Structural analyzes***

Coordinates of the 3D structures of human tissue transglutaminase 2 (PDB: 1KV3), human tissue transglutaminase 3 (PDB: 1L9M), human factor XIII (PDB: 1QRK), human NAT2 (PDB: 2PFR), *Mycobacterium abscessus* NAT (PDB: 4GUZ) and *Mesorhizobium loti* NAT1 (PDB:2BSZ) were retrieved from the Protein Data Bank. Structure were aligned, analyzed and visualized using Chimera software [25].

### ***Gaussian Network Model (GNM) calculation***

The GNM of *M. loti* NAT1 structure (PDB: 2BSZ) and human TG2 (PDB: 1KV3) were analyzed by Prody program [26,27]. Kirchhoff matrix was built firstly, with cut-off distance of 7 angstroms, and gamma value of 1.0. The slowest mode was selected for square fluctuation analysis.

## **RESULTS AND DISCUSSION**

Figure 1A shows the conservation of the Cys-His-Asp catalytic triad residues of three different active transglutaminase enzymes (including human TG2) that have been structurally aligned. This alignment also clearly indicates the structural conservation of the Trp residue (Trp 241 for human TG2) in the active site of TGs in a position close to the catalytic cysteine side chain (a distance of 5.9 Å between the thiol group of the catalytic cysteine and the Trp side chain). We also aligned the 3D structures of three well characterized and enzymatically active NATs (human NAT2, *Mycobacterium abscessus* NAT and *Mesorhizobium loti* NAT1). As shown in Figure 1B, a similar structural arrangement of the Cys-His-Asp catalytic triad and of a Phe residue (Phe42 for *M. loti* NAT1) in the active site of these enzymes was found. Moreover, in the aligned NAT structures, this Phe residue (or Trp residue for *M. abscessus* NAT) is also positioned very close to the catalytic cysteine (distance of 5.5 Å between the thiol group of Cys73 and the Phe42 side chain in *M. loti*

NAT1) as observed for the Trp residue in TGs structures (Figure 1A and 1B). Further structural alignment of the catalytic center of TGs and NAT enzymes (for clarity only human TG2 and *M. loti* NAT1 are shown in Figure 1C) supports the observation that the Phe and Trp residues occupy a very similar spatial position in the catalytic site of these two different enzymes (Figure 1C). In NATs, the Phe residue is part of a highly conserved motif (known as the “PFEN” motif) which participates to the active site pocket of NAT enzymes and contributes to the stability of their structures [28]. Multiple sequence alignment of the amino acid sequences of 41 enzymatically active eukaryotic and prokaryotic NAT enzymes clearly shows the high degree of conservation of this motif (Supplementary Figure 1). More importantly, the alignment indicates that in active NATs, only a Phe, Tyr or Trp residue is present in the motif thus strongly suggesting that an aromatic residue is needed at this position for NAT activity (Figure 1D and supplementary Figure 1). In active TG enzymes, so far, only a Trp residue has been found at this equivalent position [2,4]. However, it has been shown that Tyr could partially functionally compensate for Trp in catalysis [4]. As indicated in Figure 1E, protein flexibility analysis using Gaussian Network Model (GNM) approaches further show that the catalytic triad amino acids and the Phe/Tyr/Trp residue (referred thereafter in the manuscript as “F/Y/W” residue) of the “PFEN” motif of *M. loti* NAT1 display little flexibility (with square fluctuations below 0.1) as observed in TG enzymes (Figure 1E; for clarity only human TG2 and/or *M. loti* NAT1 square fluctuations per residue number are shown). Reduced flexibility of these catalytic residues is consistent with the need to maintain their spatial arrangement for catalysis (notably for transition state stabilization) [4,12]. As shown previously, in active TG enzymes the conserved Trp residue has been shown to be crucial for stabilization of transition state intermediates [4]. Therefore, our results reported above strongly suggest that the “F/Y/W” residue of the “PFEN” motif of NAT enzymes fulfils a role in catalysis similar to that of the active site Trp residue of

functional TGs.

Biochemical and enzymatic analyses were carried out using *M. loti* NAT1 as a model of active NAT enzymes. This NAT enzyme is well characterized both at the structural and functional level and is easily amenable to mutagenesis, heterologous expression in *E. coli*, purification to homogeneity and enzymatic assays [21,24]. In *M. loti* NAT1, the aromatic residue present in the “PFEN” motif is a Phe residue (supplementary Figure 1). Therefore, WT *M. loti* NAT1 and several mutants where the Phe42 residue was mutated to Tyr, Trp, His, Ala, or Ile were expressed in *E. Coli* as done previously with TG2 [4]. No differences in the growth and amount of *E. coli* cells were observed suggesting that no mutant was deleterious for the bacterium. All cultures (1 liter of Luria-Berthani medium) yielded ~30 mg of pure and soluble proteins excepted for the F42A mutant (~5 mg protein) which was prone to aggregation at high concentrations (>0.5 mg/ml) (Figure 2A). In order to evaluate possible structural changes due to the mutations of Phe42, far and near-UV circular dichroism (CD) spectroscopy analysis was carried out with the purified proteins. As shown in Figure 2B, the mutations had no impact on the secondary structure of the enzyme. Similarly, near-UV CD spectroscopy showed no major differences between WT *M. loti* NAT1 and the mutants, excepted for the F42W for which a small difference in molar ellipticity was observed between 290 and 310 nm due to the introduction of the Trp residue was observed (Figure 2C). Therefore, these experiments suggest that F42Y, F42W, F42H, and F42I mutant have an overall fold similar to the WT enzyme. This is in agreement with the crystal structure of the F42W *M. loti* NAT1 mutant which has been shown to fold exactly as the WT *M. loti* NAT1 enzyme [24]. As expected from the expression and purification experiments, analysis of the F42A mutant by CD gave inconsistent results due to its tendency to aggregate at high concentrations (>0,5 mg/ml). This further suggests that the presence at position 42 of a residue with a large side chain (larger than Ala) is needed for

protein integrity. This is also consistent with data indicating that amino acids of the “PFEN” motif are involved in stabilizing the structure of NAT enzymes [28].

We next tested whether the different mutants were functional using two prototypic NAT arylamine substrates, 2-aminofluorene (2-AF) and *p*-aminosalicylate (*p*-AS). As shown in Figure 2D, NAT activity was readily measured for WT enzyme (with a Phe at position 42), F42Y and F42W mutants. Conversely, F42H, F42I and F42A mutants displayed very poor activity. Moreover, while F42W mutant had activity similar to those of the WT enzyme, the F42Y mutant displayed activity higher than WT. These data clearly indicate that the presence of an aromatic residue at position 42 is crucial for NAT enzyme activity. This is in agreement with the strict conservation of an aromatic residue at this position in functional NAT enzymes characterized to date (Figure 1D and supplementary Figure 1).

To better evaluate the role of the F/Y/W residue of the “PFEN” motif of NAT enzymes, notably in transition-state stabilization, kinetic parameters ( $K_m$ ,  $k_{cat}$ ,  $k_{cat}/K_m$ ) were determined for the active *M. loti* NAT1 proteins (WT, F42W and F42Y) using AcCoA and PAS as model substrates. Activity of NAT enzymes occurs via a bi-bi ping pong mechanism, the initial rates were fitted to equation 1, which reflects this (see Materials and Methods and supplementary Figure 2). As substrate inhibition was observed for the F42Y mutant, the equation to which the initial rates for this mutant were fitted includes a substrate inhibition parameter (Equation 2, see Materials and Methods and supplementary Figure 2). Kinetic constants for the three *M. loti* NAT1 proteins are shown in Table 1. All enzymes were found to be highly active with  $k_{cat}$  values  $> 1 \text{ s}^{-1}$ . Notably, the  $k_{cat}$  of the F42W and F42Y were 5 and 60 times higher than those of the WT enzyme. The  $K_m$  values for AcCoA and PAS were also moderately increased by the mutations (up to 13 times for  $K_m$  AcCoA of the F42Y compared to WT). Accordingly,  $\Delta\Delta G_B$  values for AcCoA and PAS were also increased (values

ranging from 0.57 to 1.86 kcal/mol). This is in agreement with different structural studies on *M. loti* NAT1, *P. aeruginosa* NAT, *M. Abscessus* NAT, *M. Marinum* NAT, *M. smegmatis* NAT and human NAT2 showing that the F/Y/W residue interacts with the cofactor CoA and/or aromatic substrates [10,24,28-30]. Our results are also in agreement with the data obtained in TG enzymes, where substitution of the Trp residue have a greater impact on the catalytic rate constant  $k_{cat}$  than on the Michaelis constant  $K_m$  parameter [4]. Taking into account the data reported above, the catalytic efficiencies ( $k_{cat}/K_{mAcCoA}$  and  $k_{cat}/K_{mPAS}$ ) of F42W and F42Y were found to be increased compared to WT, notably for the F42Y mutant ( $k_{cat}/K_{mAcCoA}$  and  $k_{cat}/K_{mPAS}$  5 and 24 times higher than WT, respectively (Table 1). These increases in catalytic efficiency are largely attributable to increases in  $k_{cat}$  rather than decreased in  $K_m$  and are associated with reduced  $\Delta\Delta G_{TS}$  (-0.91 kcal/mol for the enzyme acetylation step and -1,53 kcal/mol for the PAS acetylation step by the F42Y mutant). Introduction of a hydroxyl and indole group in F42Y and F42W mutants may further contribute to stabilization of the transition state intermediate through hydrogen bonds as shown for TG enzymes [4]. Overall, our data indicate that the F/Y/W residue of the 'PFEN' motif of NAT enzymes is likely to be involved in transition state stabilization as shown for its counterpart in TG enzymes (Trp241 in human TG2) [4].

Although more modest than its impact on catalysis, the conserved Trp residue of TG enzymes has also been shown to contribute to formation of the Michaelis complex [4]. Accordingly, we also confirmed that the F/Y/W residue of the 'PFEN' motif of NATs also contributes to substrate binding (Table 1) [10,24,29-31]. Identification of active site residues involved in the stabilization of transition state residues is important to understand catalytic mechanisms and to develop potent inhibitors [20]. As the inhibition of bacterial NAT enzymes has been shown to be of clinical interest, our data may thus be helpful in the design of NAT inhibitors [9].

**TABLE 1: Kinetic and thermodynamic parameters for PAS acetylation by (RHILO)NAT1 WT and F42W and F42Y mutants**

Kinetic constants and  $\Delta\Delta G$  values were determined as described in Materials and Methods. Values are mean  $\pm$  SD of triplicate determinations.

$\Delta\Delta G_B$  = differences between WT and mutant enzymes in free energy required to form the Michaelis complex

$\Delta\Delta G_{TS}$  = differences between WT and mutant enzymes in free energy required to stabilize the transition-state complexes

	WT	F42W	F42Y
$k_{cat}$ ( $s^{-1}$ )	$1.36 \pm 0.61$	$6.86 \pm 1.22$	$82.12 \pm 18.14$
$K_{m(AcCoA)}$ ( $\mu M$ )	$94.11 \pm 43.5$	$404.8 \pm 125.2$	$1228.23 \pm 252.4$
$K_{m(PAS)}$ ( $\mu M$ )	$164.03 \pm 49.05$	$665.72 \pm 231.5$	$427.12 \pm 150.3$
$k_{cat}/K_{m(AcCoA)}$ ( $s^{-1}\mu M^{-1}$ )	0.014	0.017	0.067
$k_{cat}/K_{m(PAS)}$ ( $s^{-1}\mu M^{-1}$ )	0.008	0.010	0.192
$\Delta\Delta G_{B(AcCoA)}$ (kcal/mol)		0.86	1.52
$\Delta\Delta G_{B(PAS)}$ (kcal/mol)		0.83	0.57
$\Delta\Delta G_{TS(AcCoA)}$ (kcal/mol)		-0.09	-0.91
$\Delta\Delta G_{TS(PAS)}$ (kcal/mol)		-0.13	-1.53

## **ACKNOWLEDGEMENTS**

This work was supported by University Paris Diderot and CNRS. We thank the China Scholarship Council (CSC) for supporting the PhD of WZ, XX and RL. CM is supported by a PhD fellowship from Paris Diderot University (Ecole Doctorale BioSPC). All authors declare they have no conflict of interest.

## LEGENDS TO FIGURES

### Figure 1. Structural comparison of enzymatically active transglutaminases and arylamine N-acetyltransferases.

(A) Structural alignment of human TG2 (red color), human TG3 (grey color) and human factor XIII (cyan color). Catalytic triad residues (Cys-His-Asp) and the conserved Trp residue are shown.

Numbering corresponds to amino acids of human TG2.

(B) Structural alignment of human *M. loti* NAT1 (red color), *M. abscessus* NAT (grey color) and human NAT2 (cyan color). Catalytic triad residues (Cys-His-Asp) and the conserved Phe42/Trp42 (*M. loti* NAT1 and *M. abscessus* NAT, respectively) are shown.

(C) Structural alignment of the catalytic center of human TG2 (amino acids 231-372, red color) and *M. loti* NAT1 (amino acids 38-138, cyan color). The catalytic triad residues and the Trp241 and Phe42 residues of human TG2 and *M. loti* NAT1 are shown in red and cyan colors, respectively.

(D) Residue type in the 'PFEN' motif of functional NAT enzymes. The numbers were calculated from the multiple alignment of the amino acid sequence of the 41 active NAT enzymes (see supplementary Figure 1). Occurrence of Phe (F), Trp (W) and Tyr (Y) residue at the second position of the the 'PFEN' motif of NAT enzymes is shown above each bar.

(E) Residue mobility of *M. loti* NAT1 and human TG2 were calculated using Gaussian Network Model (GNM) as described in Materials and Methods. Square fluctuations of human TG2 (PDB 1KV3) and *M. loti* NAT1 (PDB 2BSZ) were generated from the slowed mode of GNM and are shown for each residue. Mean value of all the residues for each protein is drawn in dashed line. The right panel shows a cartoon diagram of *M. loti* NAT1 with color scale of residue mobility (square fluctuations ranging from dark blue to red).

**Figure 2. Heterologous expression, purification and determination of NAT activity of WT *M. loti* NAT1 and F42Y, F42W, F42H, F42I and F42A mutants.**

(A) Coomassie staining of 3  $\mu\text{g}$  of WT *M. loti* NAT1, F42Y, F42W, F42H, F42I and F42A mutants.

(B) Far-UV CD spectra (180-260 nm) of WT *M. loti* NAT1, F42Y, F42W, F42H and F42I mutants.

(C) Near-UV CD spectra (250-350 nm) of WT *M. loti* NAT1, F42Y, F42W, F42H and F42I mutants.

(D) Enzymatic activity of WT *M. loti* NAT1, F42Y, F42W, F42H, F42I and F42A mutants towards 2-AF and p-AS substrates. Data are represented as means  $\pm$  SD of triplicate experiments.

## REFERENCES

- [1] C.S. Lee, H.H. Park, Structural aspects of transglutaminase 2: functional, structural, and regulatory diversity, *Apoptosis : an international journal on programmed cell death* 22 (2017) 1057-1068. 10.1007/s10495-017-1396-9.
- [2] S.N. Murthy, S. Iismaa, G. Begg, D.M. Freymann, R.M. Graham, L. Lorand, Conserved tryptophan in the core domain of transglutaminase is essential for catalytic activity, *Proceedings of the National Academy of Sciences of the United States of America* 99 (2002) 2738-2742. 10.1073/pnas.052715799.
- [3] H. Sun, M.T. Kaartinen, Transglutaminases in Monocytes and Macrophages, *Medical sciences* 6 (2018). 10.3390/medsci6040115.
- [4] S.E. Iismaa, S. Holman, M.A. Wouters, L. Lorand, R.M. Graham, A. Husain, Evolutionary specialization of a tryptophan indole group for transition-state stabilization by eukaryotic transglutaminases, *Proceedings of the National Academy of Sciences of the United States of America* 100 (2003) 12636-12641. 10.1073/pnas.1635052100.
- [5] D.W. Hein, Molecular genetics and function of NAT1 and NAT2: role in aromatic amine metabolism and carcinogenesis, *Mutation research* 506-507 (2002) 65-77. 10.1016/s0027-5107(02)00153-7.
- [6] E. Sim, N. Lack, C.J. Wang, H. Long, I. Westwood, E. Fullam, A. Kawamura, Arylamine N-acetyltransferases: structural and functional implications of polymorphisms, *Toxicology* 254 (2008) 170-183. 10.1016/j.tox.2008.08.022.
- [7] A.E. Glenn, E.P. Karagianni, A. Ulndreaj, S. Boukouvala, Comparative genomic and phylogenetic investigation of the xenobiotic metabolizing arylamine N-acetyltransferase enzyme family, *FEBS letters* 584 (2010) 3158-3164. 10.1016/j.febslet.2010.05.063.
- [8] N. Laurieri, J. Dairou, J.E. Egleton, L.A. Stanley, A.J. Russell, J.M. Dupret, E. Sim, F. Rodrigues-Lima, From arylamine N-acetyltransferase to folate-dependent acetyl CoA hydrolase: impact of folic acid on the activity of (HUMAN)NAT1 and its homologue (MOUSE)NAT2, *PLoS one* 9 (2014) e96370. 10.1371/journal.pone.0096370.
- [9] E. Sim, G. Fakis, N. Laurieri, S. Boukouvala, Arylamine N-acetyltransferases--from drug metabolism and pharmacogenetics to identification of novel targets for pharmacological intervention, *Advances in pharmacology* 63 (2012) 169-205. 10.1016/B978-0-12-398339-8.00005-7.
- [10] A.M. Abuhammad, E.D. Lowe, E. Fullam, M. Noble, E.F. Garman, E. Sim, Probing the architecture of the *Mycobacterium marinum* arylamine N-acetyltransferase active site, *Protein & cell* 1 (2010) 384-392. 10.1007/s13238-010-0037-7.
- [11] S.J. Holton, J. Dairou, J. Sandy, F. Rodrigues-Lima, J.M. Dupret, M.E. Noble, E. Sim, Structure of *Mesorhizobium loti* arylamine N-acetyltransferase 1, *Acta crystallographica. Section F, Structural biology and crystallization communications* 61 (2005) 14-16. 10.1107/S1744309104030659.
- [12] X. Kubiak, I. Li de la Sierra-Gallay, A.F. Chaffotte, B. Pluvinage, P. Weber, A. Haouz, J.M. Dupret, F. Rodrigues-Lima, Structural and biochemical characterization of an active arylamine N-acetyltransferase possessing a non-canonical Cys-His-Glu catalytic triad, *The Journal of biological chemistry* 288 (2013) 22493-22505. 10.1074/jbc.M113.468595.
- [13] M. Martins, B. Pluvinage, I. Li de la Sierra-Gallay, F. Barbault, J. Dairou, J.M. Dupret, F. Rodrigues-Lima, Functional and structural characterization of the arylamine N-acetyltransferase from the opportunistic pathogen *Nocardia farcinica*, *Journal of molecular biology* 383 (2008) 549-560. 10.1016/j.jmb.2008.08.035.
- [14] J.C. Sinclair, J. Sandy, R. Delgoda, E. Sim, M.E. Noble, Structure of arylamine N-acetyltransferase reveals a catalytic triad, *Nature structural biology* 7 (2000) 560-564. 10.1038/76783.
- [15] I.M. Westwood, S.J. Holton, F. Rodrigues-Lima, J.M. Dupret, S. Bhakta, M.E. Noble, E. Sim, Expression, purification, characterization and structure of *Pseudomonas aeruginosa* arylamine N-acetyltransferase, *The Biochemical journal* 385 (2005) 605-612. 10.1042/BJ20041330.
- [16] H. Wu, L. Dombrovsky, W. Tempel, F. Martin, P. Loppnau, G.H. Goodfellow, D.M. Grant, A.N. Plotnikov, Structural basis of substrate-binding specificity of human arylamine N-acetyltransferases, *The Journal of biological chemistry* 282 (2007) 30189-30197. 10.1074/jbc.M704138200.
- [17] X. Xu, X. Kubiak, J.M. Dupret, F. Rodrigues-Lima, Arylamine N-acetyltransferases: a structural perspective.

Comments regarding the BJP paper by Zhou et al., 2013, British journal of pharmacology 171 (2014) 279-280. 10.1111/bph.12273.

[18] F. Rodrigues-Lima, C. Delomenie, G.H. Goodfellow, D.M. Grant, J.M. Dupret, Homology modelling and structural analysis of human arylamine N-acetyltransferase NAT1: evidence for the conservation of a cysteine protease catalytic domain and an active-site loop, *The Biochemical journal* 356 (2001) 327-334. 10.1042/0264-6021:3560327.

[19] B. Riddle, W.P. Jencks, Acetyl-coenzyme A: arylamine N-acetyltransferase. Role of the acetyl-enzyme intermediate and the effects of substituents on the rate, *The Journal of biological chemistry* 246 (1971) 3250-3258.

[20] R.A. Copeland, Evaluation of enzyme inhibitors in drug discovery. A guide for medicinal chemists and pharmacologists, *Methods of biochemical analysis* 46 (2005) 1-265.

[21] N. Atmane, J. Dairou, D. Flatters, M. Martins, B. Pluvinaige, P. Derreumaux, J.M. Dupret, F. Rodrigues-Lima, The conserved glycine/alanine residue of the active-site loop containing the putative acetylCoA-binding motif is essential for the overall structural integrity of *Mesorhizobium loti* arylamine N-acetyltransferase 1, *Biochemical and biophysical research communications* 361 (2007) 256-262. 10.1016/j.bbrc.2007.07.034.

[22] C.-B. A, *Fundamentals of Enzyme Kinetics*, 2nd edition ed., Portland Press, London 1995.

[23] A.J. Wilkinson, A.R. Fersht, D.M. Blow, G. Winter, Site-directed mutagenesis as a probe of enzyme structure and catalysis: tyrosyl-tRNA synthetase cysteine-35 to glycine-35 mutation, *Biochemistry* 22 (1983) 3581-3586. 10.1021/bi00284a007.

[24] X. Xu, I. Li de la Sierra-Gallay, X. Kubiak, R. Duval, A.F. Chaffotte, J.M. Dupret, A. Haouz, F. Rodrigues-Lima, Insight into cofactor recognition in arylamine N-acetyltransferase enzymes: structure of *Mesorhizobium loti* arylamine N-acetyltransferase in complex with coenzyme A, *Acta crystallographica. Section D, Biological crystallography* 71 (2015) 266-273. 10.1107/S139900471402522X.

[25] E.F. Pettersen, T.D. Goddard, C.C. Huang, G.S. Couch, D.M. Greenblatt, E.C. Meng, T.E. Ferrin, UCSF Chimera--a visualization system for exploratory research and analysis, *Journal of computational chemistry* 25 (2004) 1605-1612. 10.1002/jcc.20084.

[26] A. Bakan, A. Dutta, W. Mao, Y. Liu, C. Chennubhotla, T.R. Lezon, I. Bahar, Evol and ProDy for bridging protein sequence evolution and structural dynamics, *Bioinformatics* 30 (2014) 2681-2683. 10.1093/bioinformatics/btu336.

[27] A. Bakan, L.M. Meireles, I. Bahar, ProDy: protein dynamics inferred from theory and experiments, *Bioinformatics* 27 (2011) 1575-1577. 10.1093/bioinformatics/btr168.

[28] J. Sandy, A. Mushtaq, S.J. Holton, P. Schartau, M.E. Noble, E. Sim, Investigation of the catalytic triad of arylamine N-acetyltransferases: essential residues required for acetyl transfer to arylamines, *The Biochemical journal* 390 (2005) 115-123. 10.1042/BJ20050277.

[29] A. Coccagn, X. Kubiak, X. Xu, G. Garnier, I. Li de la Sierra-Gallay, L. Chi-Bui, J. Dairou, F. Busi, A. Abuhammad, A. Haouz, J.M. Dupret, J.L. Herrmann, F. Rodrigues-Lima, Structural and functional characterization of an arylamine N-acetyltransferase from the pathogen *Mycobacterium abscessus*: differences from other mycobacterial isoforms and implications for selective inhibition, *Acta crystallographica. Section D, Biological crystallography* 70 (2014) 3066-3079. 10.1107/S1399004714021282.

[30] E. Fullam, I.M. Westwood, M.C. Anderton, E.D. Lowe, E. Sim, M.E. Noble, Divergence of cofactor recognition across evolution: coenzyme A binding in a prokaryotic arylamine N-acetyltransferase, *Journal of molecular biology* 375 (2008) 178-191. 10.1016/j.jmb.2007.10.019.

[31] J. Sandy, S. Holton, E. Fullam, E. Sim, M. Noble, Binding of the anti-tubercular drug isoniazid to the arylamine N-acetyltransferase protein from *Mycobacterium smegmatis*, *Protein science : a publication of the Protein Society* 14 (2005) 775-782. 10.1110/ps.041163505.

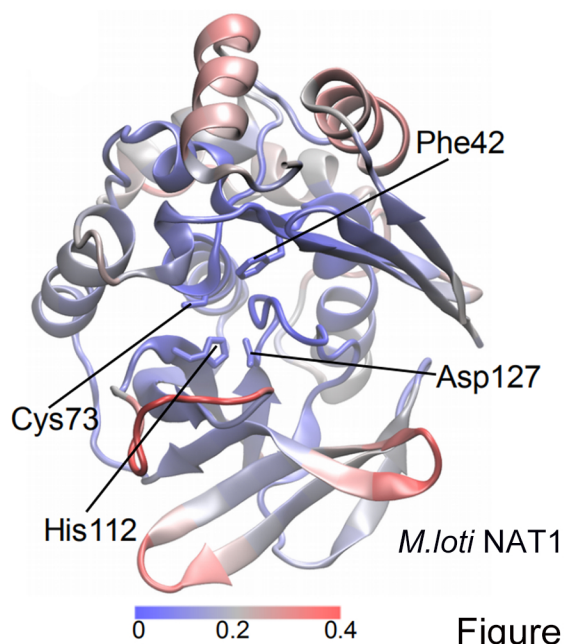
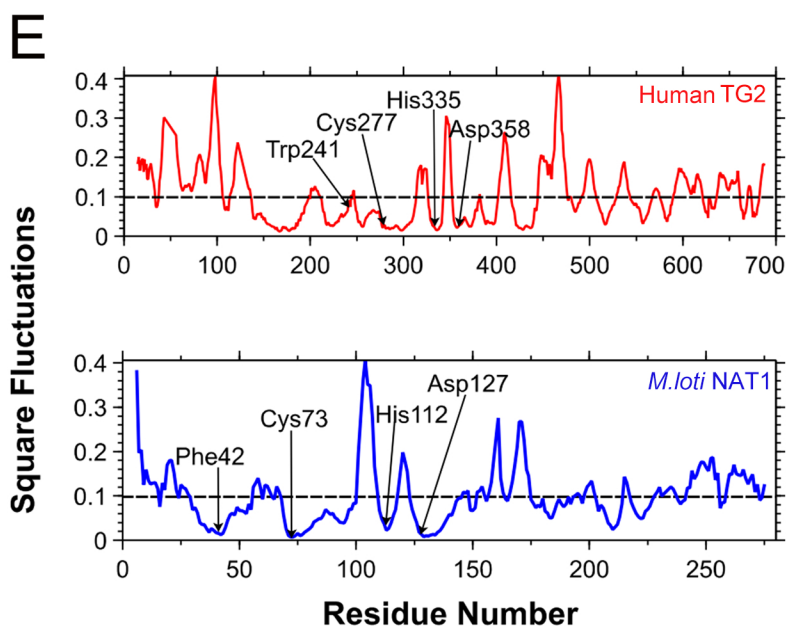
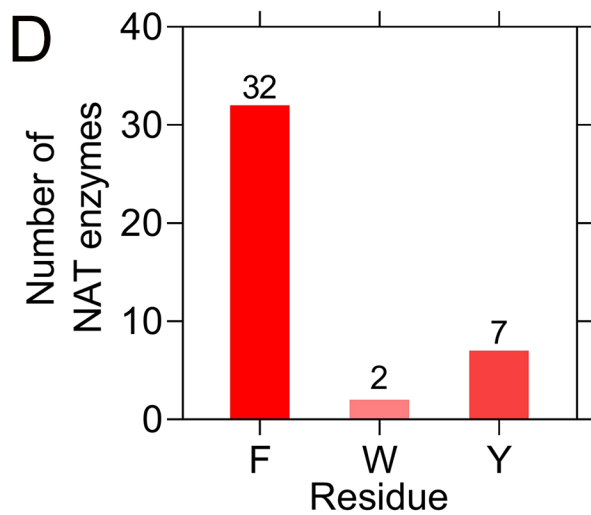
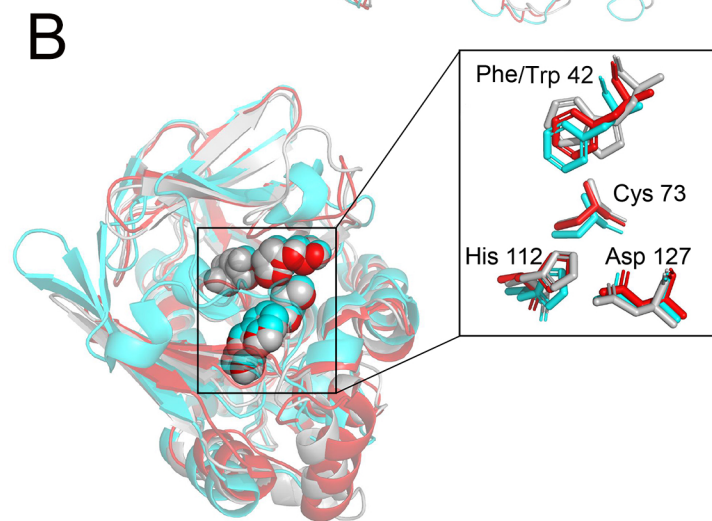
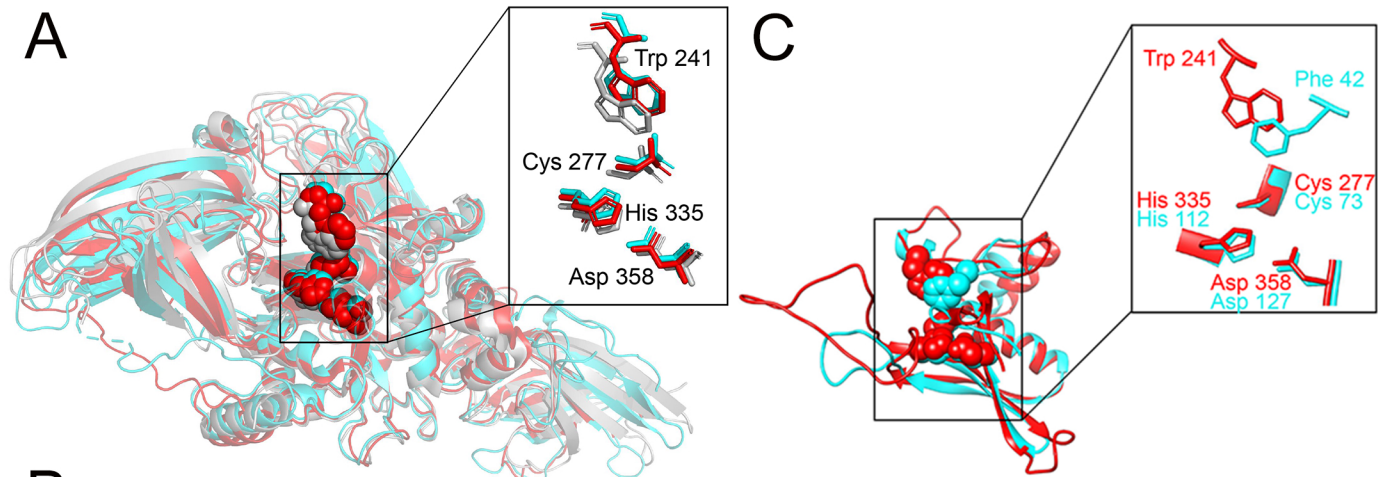


Figure 1

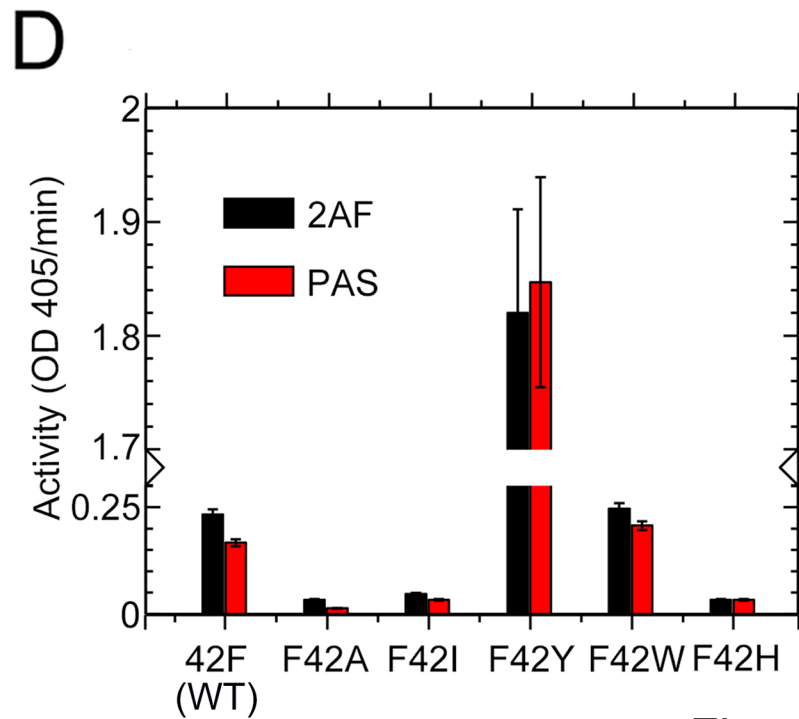
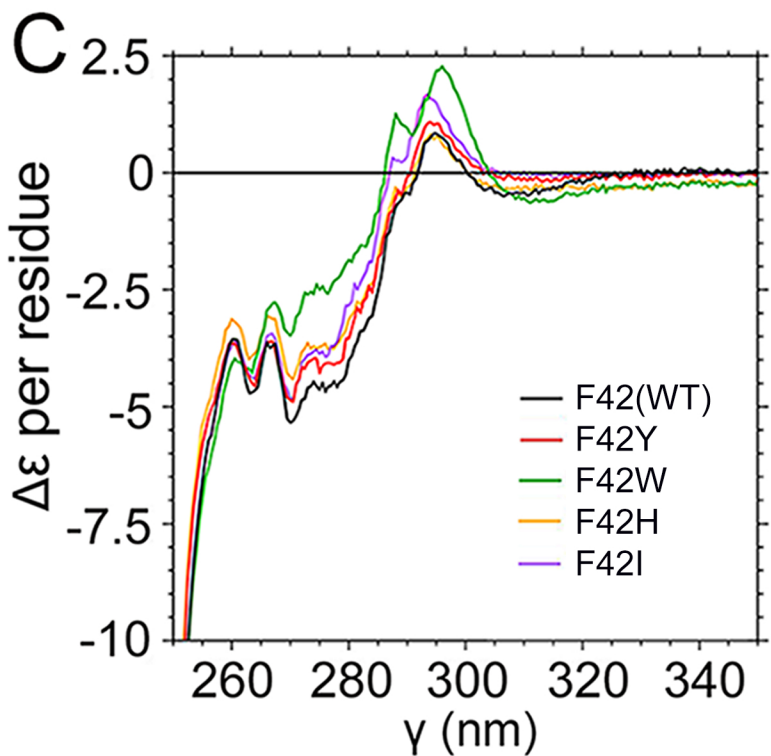
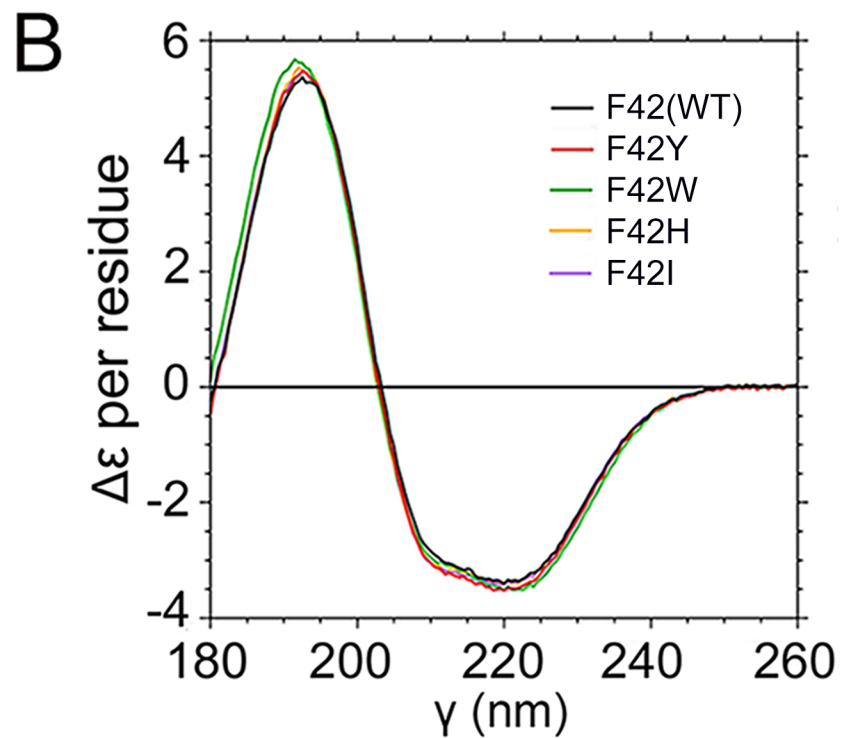
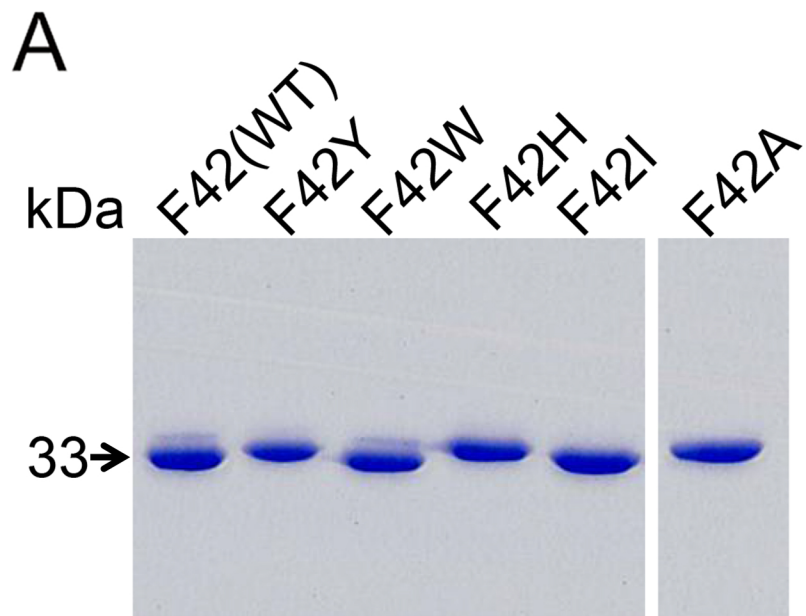


Figure 2